Title

Resonant soft X-ray scattering for polymer materials

Authors

Liu, Feng

Brady, Michael A

Wang, Cheng

Publication Date

2016-08-01

DOI

10.1016/j.eurpolymj.2016.04.014

Peer reviewed

Resonant Soft X-ray Scattering for Polymer Materials

Feng Liu,[1,2] Michael A. Brady,[1,2] Cheng Wang[1]

1. Advanced Light Source, Lawrence Berkeley National Laboratory, 1 Cyclotron Road, Berkeley, CA 94720
2. Materials Sciences Division, Molecular Foundry, Lawrence Berkeley National Laboratory, 1 Cyclotron Road, Berkeley, CA 94720

1. Introduction

The structure of materials, the way in which atoms and molecules are organized at the nano- and mesocale, determines their physical properties and functions.[1,2] In traditional crystalline materials, the atom arrangement and packing structure play a critical role in determining the mechanical behavior as well as electronic structure. In more recent developments in soft material science, it has been shown that not only the chemical structures, but also the manner that functional units are organized, is critical. Examples in this category can be found in polymer science, biomaterials, composites, and functional materials of varied applications.[3-5] However, the complexity of material architecture, chemistry, and interactions among constituent materials, for example in nano-porous/nano-crystalline materials,[6,7] functionalized nanocomposites,[3] battery electrolytes/electrodes,[8,9] organic electronics,[10,11] gas separation membranes,[12,13] fuel cell membranes,[14,15] photocatalytic materials,[16,17] and biomaterials/hybrid-biomaterials,[5,18] make it a challenging task to elucidate clear structure-property relationships. The fundamental understanding and utilization of these complex materials requires probing the physical and chemical structure-property relationship and dynamics at the molecular scale. Specialized meso-scale characterization tools and interdisciplinary understanding are required to harvest the benefits of mesoscale phenomena and functionalities. Various techniques such as scanning probe microscopy, electron microscopy, x-ray microscopy, neutron scattering, and x-ray scattering have been utilized to study these important structure-property relationships. Amongst these, x-ray scattering methods are widely used as a high resolution, nondestructive structure probe. The scattering represents a statistical average over a large sample area and therefore is complementary to direct imaging techniques such as electron microscopy and scanning

probe microscopy.[19] However, scattering contrast, and thus scattered intensity that describes heterogeneity, using conventional small angle x-ray scattering (SAXS) at hard X-ray energies (E_{ph} > 2500 eV) relies on electron density differences unless energies near an absorption edge are used to exploit “anomalous” enhancements.[20] Recently developed, resonant soft x-ray scattering (RSoXS) methods combine conventional SAXS with soft x-ray spectroscopy, thus offering enhanced and tunable scattering contrast. By tuning the x-ray photon energy close to and within the fine structure of a constituent element absorption edge, unique chemical sensitivity among components in a heterogeneous material is obtained.[20] RSoXS therefore satisfies the need for a meso-scale (nm – μm) structure probe with both elemental and chemical environment sensitivity and can have orders of magnitude scattering intensity enhancement over conventional SAXS, making it an ideal tool to study the meso-structure of heterogeneous materials. In this article we focus on the continued development of the RSoXS technique, including the principles of soft x-ray scattering, its advantages over hard X-ray scattering, and its soft materials science applications and future development.

3. RSoXS: Principles and Instrumentation

RSoXS Principles

This section will describe in detail the principles and operational mechanisms of resonant soft x-ray scattering. **Figure 1a** summarizes the basics of conventional SAXS. Unlike x-ray crystallography, SAXS measurements probe the scattering intensity variation at very small angles near the primary beam. SAXS provides structural information on the inhomogeneity of the electron density, with characteristic dimensions between a few and a few hundred nm. This method yields not only information on sizes, shapes, and distributions of particles, but also on the structure of disordered and partially ordered systems. From the first Born approximation, the scattering intensity of SAXS is the modulus-squared Fourier transformation of the electron density of the sample in real space.[21] When the x-ray energy is high and away from any absorption edges, the x-rays interact with the electrons as if they are free electrons. The scattering

is essentially a sum of the scattering from all of the individual electrons. The contrast between the heterogeneities is determined by the difference in the electron density of each material. However, when the x-ray energy is tuned near the atomic absorption edge of constituent elements, for example the K absorption edge of carbon at 284 eV, the core electron is excited to an unoccupied molecular orbital, and strong resonance enhancement in the scattering intensity is observed, relative to energies far below or above this absorption edge. Now, the x-ray is no longer interacting with 'free' electrons but bound electrons. This resonance effect is analogous to the simple harmonic oscillator: the x-ray absorption and thus scattering reach the maximum when the incident x-ray energy matches the resonant frequency of the specific chemical bond. This process is elementally sensitive, as the core-electron binding energy is elementally specific (C K edge at ~284 eV, N K edge at ~410 eV, O K edge at ~543 eV, F K edge at ~696 eV, and so on). Furthermore, this resonant process is also chemically sensitive, as the excited state that corresponds to an unoccupied molecular orbital is defined by the chemical bond environment. The anomalous scattering effect can be used to provide enhanced scattering intensity and chemical sensitivity of the scattering objects, thus resulting in the unprecedented analytical capability of a tunable, chemically sensitive structure probe of nano-scale and meso-scale components in heterogeneous, complex materials, without the need for chemical modification.[22]

The physical basis of the contrast mechanism and the general advantages of RSoXS have been demonstrated in the past few years.[23-25] The effects of the interaction of x-rays with matter are encoded in the complex index of refraction, $n(E) = 1 - \delta(E) + i\beta(E)$, where E is the photon energy, δ is the dispersive component, and β is the absorptive component.[23] These two energy dependent terms of the index of refraction are related to the complex scattering factor, $f = f_1 + if_2 = f_0 + \Delta f' + i\Delta f''$, in the forward scattering or long wavelength limit, through $\delta + i\beta = \alpha\lambda^2(f_1 + if_2)$, where $\alpha = n_a r_e/2\pi$, with n_a being the number density of atoms and r_e the classical radius of the electron. Consequently, bond-specific contrast can be achieved in the same manner as done in near edge x-ray absorption fine structure (NEXAFS) spectroscopy, because δ and β change rapidly as a function of photon energy near absorption edges, and the quantity $\Delta\delta^2+\Delta\beta^2$ determines the materials contrast and scattering strength. **Figure 1b** depicts the fundamental

relations as well as the physical mechanism exploited in anomalous scattering and the energy dependent optical constants δ and β for polystyrene (PS) and poly(methyl methacrylate) (PMMA). It can be seen that the difference in chemical constitution between PS and PMMA, two polymers with very similar elemental makeup and electron density but slightly different functional group chemistry, leads to drastic spectral differences, especially when the photon energy is close to 285 eV. δ and β are related to each other by the Kramers-Kronig transformation, and the material contrast between PS and PMMA can be calculated in this manner. The contrast factor is an energy dependent profile, in which the strong absorption associated with each specific bonding resonance (*e.g.* C=C, C=O) will generate very large enhancements at specific energies, which brings tunable chemical sensitivity to RSoXS. This unique chemical sensitivity of RSoXS was demonstrated in resolving the complicated morphology of a PI-*b*-PS-*b*-P*2*VP triblock copolymers (BCPs),[26] which will be discussed in detail in the application section.

Recent developments on soft x-ray scattering with polarized x-rays highlight one of the most exciting and most novel capabilities of RSoXS methods, namely the generated polarization dependent anisotropic scattering that reveals *local* molecular orientation.[27,28] In soft x-ray scattering, the linear dichroic absorption often exploited in NEXAFS or x-ray microscopy is accompanied by strong linear dichroic dispersion near the carbon absorption edge. This leads to strong scattering contrast based on bond orientation, which cannot be achieved with hard x-ray or neutron scattering, as neither hard x-rays nor neutrons have any sensitivity to bond-orientation. The use of linear or circularly polarized x-rays allows the bond orientation contrast to be switched on and off, respectively, which is very useful for characterization of the correlated and individual domain size and any long-range domain correlations.[28] The contrast factor varies at a given photon energy when the angle between a molecular transition dipole moment and incident photon electric field changes. A maximum in the contrast factor is seen when the incident photon electric field is perpendicular in vector to the transition dipole moment, associated with the specific incident photon energy, of one component in the heterogeneous material, which will lead to anisotropy in the observed scattering pattern.

Crystalline, semi-crystalline and liquid-crystalline organic materials have locally large anisotropic bond orientation statistics. This anisotropy strongly impacts the mechanical, optical, and electronic properties of such materials. For example, charge transport in organic thin films is often highly anisotropic, and the energetics of transport depend upon domain size, degree of order within domains, domain correlations, and the domain boundaries.[28] Knowing the relative impact of all ordering at these different length scales is necessary for a detailed understanding of organic thin film devices. By taking advantage of the polarization of the incident beam, an inherent characteristic of synchrotron sources, the orientation of molecular planes at surfaces and interfaces can be determined independently, providing yet another key to unlock structure-property relationships that will lead to better material design. In addition, the RSoXS instrument described in this report further provides polarization tunability through the third generation synchrotron with elliptically polarized undulator that enables modulation of the electric field vector at all angles between and including *s* and *p* polarization, as well as left and right circular polarization. Furthermore, RSoXS reveals local molecular alignment independent of overall crystallinity and represents an important new tool for examining the connection between transport properties and morphology in organic and hybrid organic-inorganic electronic devices. These correlations are valuable to guide molecular design for improved polymers and to develop a better understanding of charge generation at polymer-polymer interfaces.

RSoXS Instrumentation

Unlike the hard x-ray scattering that has been around for nearly a century, the development of soft x-ray scattering has taken place only in the last decade and primarily within the previous five years. Most of the initial soft x-ray synchrotron applications have focused on spectroscopy and were later extended to microscopy. Much of the early work, as discussed above, has largely focused on organic materials, especially thin films of conjugated polymers, polymer blends, and block copolymers.[20,23-28] Due to the organic nature of these materials, this early work has primarily utilized incident x-rays of low energy close to the carbon, nitrogen, oxygen, and fluorine 1s absorption edges. There has, however, been even earlier development using soft x-ray

scattering on magnetic materials and on strongly correlated materials where the electron ordering is of interest.[29,30]

The resonant soft x-ray scattering (RSoXS) instrument, at Beamline 11.0.1.2 at the Advanced Light Source at Lawrence Berkeley National Laboratory (LBNL), is the world's first dedicated soft x-ray scattering beamline that is optimized for meso-scale soft material science.[20,31] Sourced by a state-of-the-art elliptically polarized undulator, the scattering chamber is designed to accommodate various scattering geometries with customizable sample environments (**Figure 2a**). It is capable of collecting scattered x-ray radiation with energies from 150 eV to 1.5 keV, with full polarization control, and thus can probe a large range of heterogeneous length scales from 0.5 nm to 5 μm (**Figure 2b**), which is comparable to (or often larger than) the *q*-range that traditional SAXS and small angle neutron scattering (SANS) can access. Due to the longer wavelength, in general soft x-rays can access lower *q* values which enables the characterization of larger structure. Moreover, the flexible geometry of the scattering chamber enables numerous scattering and spectroscopy experiments. Since the samples reside on a flat plate that is attached to a goniometer (?), the plate can be tilted by 90□ to transition from a transmission SAXS setup to grazing incidence SAXS with soft x-rays (GI-RSoXS). In addition, the CCD detector can be centered at a position of 2□, and resonant soft X-ray reflectivity (RSoXR) can be performed on thin films to study buried interfaces and the chemically sensitive composition through the thickness of the film.[23] Finally, NEXAFS spectroscopy can be carried out using this RSoXS instrument, such that the spectra and scattering may be recorded with consistency. Attached to the CCD is a photodiode, where the beam transmitted through the sample is recorded as a function of photon energy to elucidate at which energies the x-rays are absorbed most, producing an inverted NEXAFS spectra. Alternatively, the sample plate may again be tilted so that total electron yield (TEY) detection of NEXAFS spectra is possible, by way of measurement of a replacement current by an electrical circuit that keeps the total charge on the sample plate neutral.

Like SAXS/WAXS, RSoXS also has the potential to be a high-throughput characterization method, where samples can be prepared on various commercially available substrates or supports (**Figure 2c**). The current sample holder can take ~50 samples with one load into the high vacuum scattering chamber (~10^{-7} torr), enabling fast screening of samples prepared by varied processing conditions. RSoXS provides a novel route to unambiguously decipher the complex morphologies of mesocale materials. Using soft X-rays, where the photon energy can be tuned to match the absorption spectrum of the different chemical components, the scattering contributions from the individual components can be isolated, enabling a glimpse into these complex morphologies with unprecedented detail. Exciting progress has been made using RSoXS in material characterization; with continuous instrumentation development and the ability to robotically measure many combinatorial samples in a high-throughput fashion, or alternatively to perform detailed time-resolved, *in operando* experiments,, the exploration of mesoscale material science will be extended to a broader scientific community, addressing the grand challenges in energy, biology, and environmental research.

3. RSoXS: Applications

RSoXS at Beamline 11.0.1.2 at the Advanced Light Source has been widely used in characterizing the morphology of thin film materials since its construction and continues to do so. RSoXS attracts users with a broad range of backgrounds, with research covering polymer, block copolymer, and composite morphology, particle assembly, organic photovoltaic morphology, organic LEDs, membranes and porous mateirals, batteries and fuel cells, biomaterials, and so on. In conjunction with complimentary techniques such as x-ray diffraction (providing crystalline information) and transmission electron microscopy (real space image and phase information), a thorough description of the structure of investigated material can be obtained. In the subsequent section, we discuss the important results of RSoXS in materials science research.

3.1. Complex Structure Determination and Chemical Sensitivity

Enhanced contrast by anomalous scattering makes RSoXS an effective tool to

characterize the morphology of thin films (~100 nm thickness) in a transmission geometry. Thus, it is widely used in studying the length scale of phase separation of block copolymers and polymer blends. One of the unique advantages of RSoXS is the chemical sensitivity as compared to conventional SAXS and SANS, and therefore the morphology of multicomponent systems of two phases and more can be resolved. One successful example is to use RSoXS to unambiguously decipher the complex morphologies of triblock copolymers (BCPs), which display morphologies that are quite complicated and can hardly be resolved by common scattering methods. Poly(*1,4*-isoprene)-*block*-polystyrene-*block*-poly(*2*-vinlypyridine) triblock copolymer (IS2VP), with chemical structure, composition and molecular weight information shown in **Figure 3a**, was chosen as the model system to carry out the experiment.[26] In hard x-ray small angle scattering, a hexagonally packed cylindrical structure was seen for this block copolymer (**Figure 3b**). However, due to the similarity in electron density among these blocks, it is not possible to distinguish different polymer phases. Using soft X-rays at the carbon K edge (near 284 eV), where the spectroscopic signatures of the polymers are dependent on the chemical composition and bonding environment, RSoXS can distinguish between different polymer species with their differences in their energy dependent complex index of refraction, which is elementally and chemically specific. Shown in **Figure 3c** is the real and imaginary components of the complex index of refraction of PS, PI, and P2VP. Since the difference in complex index of refractions is proportional to the x-ray scattering power of the materials, and when tuning the soft x-ray energy to match the absorption spectrum of the different components in the BCP, the scattering contributions from the different polymer blocks can be isolated, analogous to contrast matching in neutron scattering, but without the requirement for chemical labeling. Shown in **Figure 3d** are the transmission scattering images at three different energies and morphology model of the block copolymer, which includes the change in contrast among the three blocks as the photon energy is changed. When the photon energy is tuned to 250 eV, the dispersive component δ of PI and PS were matched, and therefore the x-rays cannot distinguish the difference between these two components. Thus, the scattering contribution of P2VP was isolated, and the scattering pattern corresponds to the distribution of the P2VP blocks. At 284 eV, the contrast between PI

and P2VP were matched, and the x-rays see a hexagonally packed cylindrical structure, which has smaller unit cell spacing. When the energy was tuned to 280 eV, the contrast was not matched for any pairs; therefore, the scattering has contributions from both domain correlations of varied unit cell spacing. RSoXS made it possible to unambiguously determine the co-assembly of two nested hexagonally packed arrays of nanoscopic cylindrical microdomains. It enabled an unequivocal evaluation of the details of their complex microphase separated morphologies and agrees with preferential staining experiments done by transmission electron microscopy (TEM). It should also be noted that the radially averaged RSoXS profiles provide far more information on this nested hexagonally packed structure as compared to hard x-ray SAXS results, due to the added benefit from anomalous scattering and spectroscopic contrast within the fine structure of the carbon 1s absorption edge.

Another descriptive example can be seen in the structural elucidation of mesoporous polymer membranes, which have application in water filtration, gas separation, and Li-ion battery electrolytes.[32,33] When hard x-ray SAXS is applied to study these films, the pores and material contrast dominate the scattering profiles, making it hard to probe detailed polymer phase separated structure. Taking polystyrene-*block*-polyethylene-*block*-polystyrene (SES) as an example,[33] hard x-ray scattering can resolve the porous structure, as indicated by the black line in **Figure 3e**. RSoXS, however, provides a much better solution to study the morphology of these samples. By taking the NEXAFS spectra of the constituent blocks and calculating the contrast between each block, block and void fractions can be calculated from the scattering results (**Figure 3f**). Therefore, through the selection of the appropriate photon energy, complementary information regarding the porous structure and polymer phase separation can be obtained.

3.2. Scattering Anisotropy and Interfacial Orientation

RSoXS has been extensively used in characterizing morphology of the active layer in thin film electronic devices. For example, RSoXS has been established as a standard method to study the length scale of phase separation in organic photovoltaics.[34] The

successful use of RSoXS has led to important discoveries in the OPV field, yielding new concepts such as multi-length-scaled morphology,[35,36] hierarchical structure,[37] phase purity and interfacial orientation,[28,38-41] strongly broadening the understanding of structure-property relationship in functional material blends. In addition to the routine application in characterizing the length scale of phase separation, the inherent feature of the polarized electric field of synchrotron soft x-rays has also been intensively exploited (polarized soft x-ray scattering, P-SoXS), providing new methodologies to study the local molecular orientation and structure and orientation at buried interfaces in polymeric thin film blends.[28] One thing to note is that polarization is the nature of the synchrotron x-rays, which means all the RSoXS experiment were utilizing polarized soft x-rays. The use of yet another acronym, P-SoXS, for this method is to emphasize the unique scattering anisotropy caused by locally ordered structure. As an example, shown in **Figure 4a** are transmission RSoXS profiles of DPP-based conjugated polymer:PCBM blends (DPP:PCBM) at different photon energies across the carbon 1s edge using horizontally polarized x-rays (*s* polarization).[40,42] DPP:PCBM blends form large-scaled PCBM aggregates, embedded in the DPP polymer matrix. The size scale of this phase separation can be directly obtained by calculation from the soft x-ray SAXS profile. As seen from **Figure 4a**, the change in photon energy leads to drastically different scattering anisotropy, with the azimuthal dependence of the scattering intensity changing at a given *q* vector. The polymer 1s-π* transition shows intensity enhancement in the vertical direction, while the 1s-σ* transition shows intensity enhancement in the horizontal direction. It was discussed previously how the transition dipole moment vector and the electric field vector alignment will lead to differences in scattering contrast factors (**Figure 4b**), which is what gives rise to this scattering anisotropy. Varying the electric field in different directions will change the anisotropy of scattering accordingly. This information was used to reconstruct the DPP polymer chain orientation with respect to the aggregated PCBM domains in the blends. It has been shown with GIWAXS that DPP is a well-ordered polymer that takes on an edge-on orientation and tends to form fibrils in bulk heterojunction blends. Thus a fibrillar mesh network morphology is expected in BHJ blends. The optical model and contrast factor from other conjugated polymer blends show that when the transition dipole moment is

aligned with the electric field, the scattering contrast factor will decrease. Thus, under *s* polarization a vertically enhanced intensity indicates that some 1s-π* transition dipoles are parallel to the x-ray electric field (**Figure 4c**). In this case the polymer chain will be aligned in the same direction as that of the fibril long axis, which is drastically different from the state-of-the-art P3HT chain organization in their fibrils (**Figure 4d**). This unique characterization capability will fundamentally change the transport picture of conjugated polymers, which show anisotropic charge transport in which hopping through the π-π stacking direction and intrachain transport are the directions of higher mobility.

This property of characterizing the local orientation is advantageous and can be applied to examine many complex structures. A successful example is demonstrated that uses linearly polarized x-rays to investigate the hierarchical structure in molecular liquid crystals.[43] Shown in **Figure 4e** is an example of a bent-core liquid crystalline molecule (NOBOW). It is known that introducing molecular chirality into a liquid crystal may lead to a twisting force that can modify the equilibrium state, resulting in various helical structures. However, achiral molecules have also been observed to form helical structures, forming the helical nanofilament (HNF) phase. The NOBOW molecule is a bent-core molecule and it is achiral, which also forms a chiral-like liquid crystal structure. This HNF is made up of twisted layers, indicating not only molecular chirality but also layer chirality drives the formation of helical structures. The helical pitch can be readily characterized using polarized RSoXS methods, yielding new understanding towards hierarchically structured materials. The scattering intensity anisotropy correlated well with the molecular dipole and x-ray electrical field interaction, which deceases when the photon energy is switched off-edge. The helical pitch expanding under thermal treatment can be easily probed by RSoXS experiments.[43]

3.3. Solvent Environment and Contrast Matching

The implementation of solution environment sample cells dramatically extends the applications of RSoXS, also considering that more sample environments can be designed for dynamic experiments of devices in operation. More importantly, it opens the possibility to study the structure of biomaterials, which have specific, inherent

functions in the solution state. Shown in **Figure 5a** is the solution cell that was developed for RSoXS, in which the liquid sample is captured in a small volume in between two silicon nitride windows that are attached with epoxy. The contrast of RSoXS can be continuously tuned by changing the photon energy, and thus biomaterials with specific functional groups can be probed, enabling the exploration of new science from natural materials. An interesting example in this category can be the found in the recent investigations of the colloidal structure of cow's milk.[44,45] Previous research has shown in specially treated dry milk that the colloidal casein supramolecule aggregated and casein polymer chains act together to maintain casein micelle integrity. The proteins aggregate into spheres of 8 nm in diameter, and calcium phosphate clusters are also present that are 4.8 nm in diameter, as shown in **Figure 5b**.[45] RSoXS of milk samples were carried out in liquid form by using the solution sample cell just described. Typical absorption profiles and reduced scattering patterns using calcium L-edge photon energies are shown in **Figure 5c**.[46] It is shown that the calcium phosphate nanoclusters display distinct absorption peaks near 350 eV, and therefore energies within the fine structure of this edge can be used to tune contrast and locate the calcium phosphate component. By tuning the photon energies, different contributions from protein aggregates and calcium phosphate clusters can be obtained. The morphology picture of casein in milk is now that the calcium phosphate clusters and protein spheres aggregate together to form a hierarchical structure, for which the inter-globular distance is around hundreds of nanometers in solution, and the calcium phosphate clusters has a inter particle distance of ~ 15 nm.

Another successful demonstration is seen in characterizing the hierarchical structure of ion-conducting polymers.[47] Nafion is the benchmark material for proton exchange membranes due to its remarkable conductivity and good structural and chemical stability.[48,49] The presence of multiple interfaces between the polymer and inorganic components can result in a preferential orientation of ion-conducting domains due to wetting interactions and ultimately affect the transport properties.[50,51] Hard x-ray SAXS lacks the capability to probe the small difference between the heterogeneous domains of this type of membrane due to the limited contrast from materials of similar density with different molecular orientation. RSoXS can maximize the contrast between phases

of interest by tuning the incident x-ray energy. Preliminary RSoXS results with a wet sample cell have demonstrated that Nafion films contain partially oriented molecules inside ionomer domains (**Figure 5d,e**). It was the first observation that before the crystalline phase starts forming, fluorine aggregation occurs in the as-cast Nafion films. Using polarized x-rays, it was surprising to observe strong scattering anisotropy, which indicated preferred local crystalline grain orientation at the interface between different phases (**Figure 5d**). This effect is only visible when tuning the photon energy to the fluorine absorption edge (~696 eV). We will further develop RSoXS with *in-situ*/*in-operando* sample environments to characterize the morphology of this class of mesoporous polymer membranes and to establish dynamical structure-property relationships under operating conditions. RSoXS is the only tool to date that can reveal this type of partial ordering within domains, a property that is important to the tuning of proton conductivity and gas permeability of photocatalytic systems, and to optimize the performance of solar-powered fuel generators.

3.4. Grazing Incidence Scattering and Depth Information

Internal thin film structures, particularly interfaces between different materials, are often critical to material properties and performance, but buried interfacial characterization is typically very difficult. Grazing incidence resonant soft x-ray scattering (GI-RSoXS), a technique that measures diffusely scattered soft X-rays to selectively reveal the spatial frequency distribution of internal interfaces, is of high interest to address this issue. With this technique, diffuse scattering from a buried interface can be selected by judicious choice of photon energy, thus allowing detailed characterization of the interfacial structure,[20] which is nearly impossible to achieve by conventional characterization methods. Taking a polymer bilayer as an example, conventional grazing incidence scattering can typically only isolate the surface and the bulk;[19] the bilayer is seen as a single layer. It is true that, by modifying the lower layer using deuteration, the buried interface can be probed by neutron scattering.[52,53] However, the cost is high and deuteration for many materials is difficult to achieve synthetically. Soft x-ray and neutron reflectivity can probe the buried interfacial information and construct vertical composition profiles of a thin film, yet they cannot reveal in-plane correlations within a

system.[53,54] Soft x-rays have relatively long wavelengths, energy dependent contrast and tunable penetration, making GI-RSoXS a very promising tool for probing nanostructured thin films. The contrast/sensitivity of the scattering pattern varies significantly with photon energy close to the absorption edge of the constituent atoms. GI-RSoXS offers extra capacities such as enhanced interfacial sensitivity and depth profiling with chemical information. The fine absorption spectra near the absorption edge due to the different chemical bonding environments allow the tuning of sensitivity by simply changing photon energy.[55] Control of the electric field intensity throughout the depth of the film and scattering contrast between materials can unambiguously identify scattering from different sources. Combined with index matching, the energy tunability can be applied to probe buried interfacial structure at different depths. We have started the general method development of GI-RSoXS with block copolymer thin films and organic photovoltaic (OPV) materials. Soft x-ray scattering data are collected as a function of incident angle, and photon energy, which should be selected to provide depth information and resonant enhancement for the different polymer components. Shown in **Figure 6a** is the GI-RSoXS of the IS2VP triblock copolymer. In the scattering image, the in-plane direction signal reveals the lateral order of the film, and the out-of-plane direction signal reveals vertical information of the thin film. In-plane line-cuts of the scattering signal are also plotted. By tuning photon energy, different blocks of the triblock copolymer can be highlighted. **Figure 6b** displays the GI-RSoXS results of a mesoporous block copolymer thin film. Quite different scattering signals at different photon energies are seen. Analysis and reconstruction of the 3-dimensional structure of the sample is currently in progress. By carefully tuning the photon energy and incidence angle, depth-dependent morphology of thin films can be studied by GI-RSoXS. **Figure 6c** depicts a typical experiment of this nature, exploring the 3-D morphology of a PS-b-P2VP block copolymer thin film.[56] A complete characterization of depth-dependent morphology would need to reduce the scattering contribution of the film interfaces, and this can be done by using the right photon energy to minimize the interface scattering effects, achieved by matching the index of refraction between the film and silicon substrate. Scattering within the soft x-ray region has the added benefit of large critical angles, thus enabling fine-tuning of this variable, offering a precise control in depth

resolution. In the PS-*b*-P2VP case, it was seen that the as cast polymer thin film showed a lamellar morphology throughout the entire film. Thermal annealing significantly reduced the ordering at the top surface to a depth about 30 nm, and the order at the thin film-substrate interface was preserved. A relevant metrology application of this scattering instrument and technique in probing the 3-D structure of soft matter is critical-dimension small-angle x-ray scattering (CD-SAXS). When a soft x-ray source is used, the enhanced contrast can be used to probe the 3-D structure of ultra thin films. Illustrated in **Figure 6d** is an example of resonant CD-SAXS (res-CDSAXS) to study the internal structure of self-assembled block copolymer thin films.[57] By taking transmission scattering measurements at variable angles, the 2-D or 3-D reciprocal space map from nanostructured scatters can be constructed, which can be further used to resolve the complex buried features in the phase separated block copolymer.

5. Conclusion

In this report, we have reviewed technical details, achievements, and future developments of resonant soft x-ray scattering. The unique advantages of RSoXS, including chemically sensitive contrast tuning, large range of accessible length scales, inherent polarization, and high throughput sample screening, make it an ideal tool for the next generation in soft matter characterization. With more soft x-ray facilities commissioned at synchrotron facilities, RSoXS will be accessible to the broader variety of user communities of different backgrounds, which will further diversify the application of this technique. We expect RSoXS to make significant contributions to understand detailed structure-property relationship in varied disciplines of materials science in the near future.

Acknowledgements

The Advanced Light Source is supported by the Director, Office of Science, Office of Basic Energy Sciences, of the U.S. Department of Energy under Contract No. DE-AC02-05CH11231.

References:

(1) Crabtree, G. W.; Sarrao, J. L. *MRS Bulletin* **2012**, *37*, 1079–1088.
(2) Barth, J. V.; Costantini, G.; Kern, K. *Nature* **2005**, *437*, 671–679.
(3) Kao, J.; Thorkelsson, K.; Bai, P.; Rancatore, B. J.; Xu, T. *Chem. Soc. Rev.* **2013**, *42*, 2654.
(4) Liu, F.; Gu, Y.; Shen, X.; Ferdous, S.; Wang, H.-W.; Russell, T. P. *Prog. Polym. Sci.* **2013**, *38*, 1990–2052.
(5) Meyers, M. A.; Chen, P.-Y.; Lin, A. Y.-M.; Seki, Y. *Prog. Mater. Sci.* **2008**, *53*, 1–206.
(6) Zhu, Q.-L.; Xu, Q. *Chem. Soc. Rev.* **2014**, *43*, 5468–5512.
(7) Tao, A. R.; Habas, S.; Yang, P. *Small* **2008**, *4*, 310–325.
(8) Hallinan, Jr., D. T.; Balsara, N. P. *Annu. Rev. Mater. Res.* **2013**, *43*, 503–525.
(9) Lee, H.; Yanilmaz, M.; Toprakci, O.; Fu, K.; Zhang, X. *Energy Environ. Sci.* **2014**, *7*, 3857-3886.
(10) Salleo, A.; Kline, R. J.; DeLongchamp, D. M.; Chabinyc, M. L. *Adv. Mater.* **2010**, *22*, 3812–3838.
(11) Liu, F.; Gu, Y.; Jung, J. W.; Jo, W. H.; Russell, T. P. *J. Polym. Sci., Part B: Polym. Phys.* **2012**, *50*, 1018–1044.
(12) Bernardo, P.; Drioli, E.; Golemme, G. *Ind. Eng. Chem. Res.* **2009**, *48*, 4638–4663.
(13) Yampolskii, Y. *Macromolecules* **2012**, *45*, 3298–3311.
(14) Steele, B. C. H.; Heinzel, A. *Nature* **2001**, *414*, 345–352.
(15) Bose, S.; Kuila, T.; Nguyen, T. X. H.; Kim, N. H.; Lau, K.-T.; Lee, J. H. *Prog. Polym. Sci.* **2011**, *36*, 813–843.
(16) Tong, H.; Ouyang, S.; Bi, Y.; Umezawa, N.; Oshikiri, M.; Ye, J. *Adv. Mater.* **2012**, *24*, 229–251.
(17) Kudo, A.; Miseki, Y. *Chem. Soc. Rev.* **2009**, *38*, 253-278.
(18) Beniash, E. *WIREs Nanomed. Nanobiotechnol.* **2011**, *3*, 47–69.
(19) Renaud, G.; Lazzari, R.; Leroy, F. *Surf. Sci. Rep.* **2009**, *64*, 255–380.
(20) Gann, E.; Young, A. T.; Collins, B. A.; Yan, H.; Nasiatka, J.; Padmore, H. A.; Ade, H.; Hexemer, A.; Wang, C. *Rev. Sci. Instrum.* **2012**, *83*, 045110.
(21) Lifshin, E. *X-ray Characterization of Materials*; John Wiley & Sons, 2008.
(22) Attwood, D. *Soft X-Rays and Extreme Ultraviolet Radiation*; Cambridge University Press, 2007.
(23) Wang, C.; Araki, T.; Ade, H. *Appl. Phys. Lett.* **2005**, *87*, 214109.
(24) Swaraj, S.; Wang, C.; Yan, H.; Watts, B.; Lüning, J.; McNeill, C. R.; Ade, H. *Nano Lett.* **2010**, *10*, 2863–2869.
(25) Virgili, J. M.; Tao, Y.; Kortright, J. B.; Balsara, N. P.; Segalman, R. A. *Macromolecules* **2007**, *40*, 2092–2099.
(26) Wang, C.; Lee, D. H.; Hexemer, A.; Kim, M. I.; WWei, Z.; Hasegawa, H.; Ade, H.; Russell, T. P. *Nano Lett.* **2011**, *11*, 3906–3911.
(27) Mannsfeld, S. C. B. *Nat. Mater.* **2012**, *11*, 489–490.
(28) Collins, B. A.; Cochran, J. E.; Yan, H.; Gann, E.; Hub, C.; Fink, R.; Wang, C.;

Schuettfort, T.; McNeill, C. R.; Chabinyc, M. L.; Ade, H. *Nat. Mater.* **2012**, *11*, 536-543.
(29) Abbamonte, P.; Rusydi, A.; Smadici, S.; Gu, G. D.; Sawatzky, G. A.; Feng, D. L. *Nat. Phys.* **2005**, *1*, 155–158.
(30) Fink, J., Schierle, E., Weschke, E., & Geck, J. (2013). *Reports on Progress in Physics*, 76(5), 056502.
(31) Carpenter, J. H.; Hunt, A.; Ade, H. *J. Electron. Spectrosc. Relat. Phenom.* **2015**, *200*, 2–14.
(32) Wong, D. T.; Wang, C.; Pople, J. A.; Balsara, N. P. *Macromolecules* **2013**, *46*, 4411–4417.
(33) Wong, D. T.; Wang, C.; Beers, K. M.; Kortright, J. B.; Balsara, N. P. *Macromolecules* **2012**, *45*, 9188–9195.
(34) Ade, H. *Eur. Phys. J. Spec. Top.* **2012**, *208*, 305–318.
(35) Liu, F.; Wei, Z.; Tumbleston, J. R.; Wang, C.; Gu, Y.; Wang, D.; Briseno, A. L.; Ade, H.; Russell, T. P. *Adv. Energy Mater.* **2014**, *4*, 1301377.
(36) Gu, Y.; Wang, C.; Russell, T. P. *Adv. Energy Mater.* **2012**, *2*, 683–690.
(37) Chen, W.; Xu, T.; He, F.; Wang, W.; Wang, C.; Strzalka, J.; Liu, Y.; Wen, J.; Miller, D. J.; Chen, J.; Hong, K.; Yu, L.; Darling, S. B. *Nano Lett.* **2011**, *11*, 3707–3713.
(38) Ma, W.; Tumbleston, J. R.; Wang, M.; Gann, E.; Huang, F.; Ade, H. *Adv. Energy Mater.* **2013**, *3*, 864–872.
(39) Collins, B. A.; Li, Z.; Tumbleston, J. R.; Gann, E.; McNeill, C. R.; Ade, H. *Adv. Energy Mater.* **2013**, *3*, 65–74.
(40) Liu, F.; Wang, C.; Baral, J. K.; Zhang, L.; Watkins, J. J.; Briseno, A. L.; Russell, T. P. *J. Am. Chem. Soc.* **2013**, *135*, 19248–19259.
(41) Mezger, M.; Jérôme, B.; Kortright, J. B.; Valvidares, M.; Gullikson, E. M.; Giglia, A.; Mahne, N.; Nannarone, S. *Phys. Rev. B* **2011**, *83*, 155406.
(42) Liu, F.; Gu, Y.; Wang, C.; Zhao, W.; Chen, D.; Briseno, A. L.; Russell, T. P. *Adv. Mater.* **2012**, *24*, 3947–3951.
(43) Zhu, C.; Wang, C.; Young, A.; Liu, F.; Gunkel, I.; Chen, D.; Walba, D.; Maclennan, J.; Clark, N.; Hexemer, A. *Nano Lett.* **2015**, *15*, 3420–3424.
(44) de Kruif, C. G.; Huppertz, T.; Urban, V. S.; Petukhov, A. V. *Advances in Colloid and Interface Science* **2012**, *171-172*, 36–52.
(45) McMahon, D. J.; Oommen, B. S. *Journal of Dairy Science* **2008**, *91*, 1709–1721.
(46) Ingham, B.; Erlangga, G. D.; Smialowska, A.; Kirby, N. M.; Wang, C.; Matia-Merino, L.; Haverkamp, R. G.; Carr, A. J. *Soft Matter* **2015**, *11*, 2723–2725.
(47) Gurevitch, I.; Buonsanti, R.; Teran, A. A.; Gludovatz, B.; Ritchie, R. O.; Cabana, J.; Balsara, N. P. *J. Electrochem. Soc.* **2013**, *160*, A1611–A1617.
(48) Kusoglu, A.; Modestino, M. A.; Hexemer, A.; Segalman, R. A.; Weber, A. Z. *ACS Macro Lett.* **2012**, *1*, 33–36.
(49) Modestino, M. A.; Kusoglu, A.; Hexemer, A.; Weber, A. Z.; Segalman, R. A. *Macromolecules* **2012**, *45*, 4681–4688.
(50) Chen, X. C.; Kortright, J. B.; Balsara, N. P. *Macromolecules* **2015**, *48*, 5648–5655.
(51) Schmidt-Rohr, K.; Chen, Q. *Nat. Mater.* **2007**, *7*, 75–83.
(52) Dietrich, S.; Haase, A. *Physics Reports* **1995**, *260*, 1–138.

(53) Russell, T. P. *X-ray and Neutron Reflectivity for the Investigation of Polymers*; 1990.
(54) Wang, C.; Araki, T.; Watts, B.; Harton, S.; Koga, T.; Basu, S.; Ade, H. *J. Vac. Sci. Technol., A* **2007**, *25*, 575.
(55) Ade, H.; Urquhart, S. G. In *Chemical Applications of Synchrotron Radiation: X-ray applications*; Sham, T.-K., Ed.; World Scientific, 2002; pp. 1–37.
(56) Wernecke, J.; Okuda, H.; Ogawa, H.; Siewert, F.; Krumrey, M. *Macromolecules* **2014**, *47*, 5719–5727.
(57) Sunday, D. F.; Hammond, M. R.; Wang, C.; Wu, W.-L.; DeLongchamp, D. M.; Tjio, M.; Cheng, J. Y.; Pitera, J. W.; Kline, R. J. *ACS Nano* **2014**, *8*, 8426–8437.

Figures and Figure Captions:

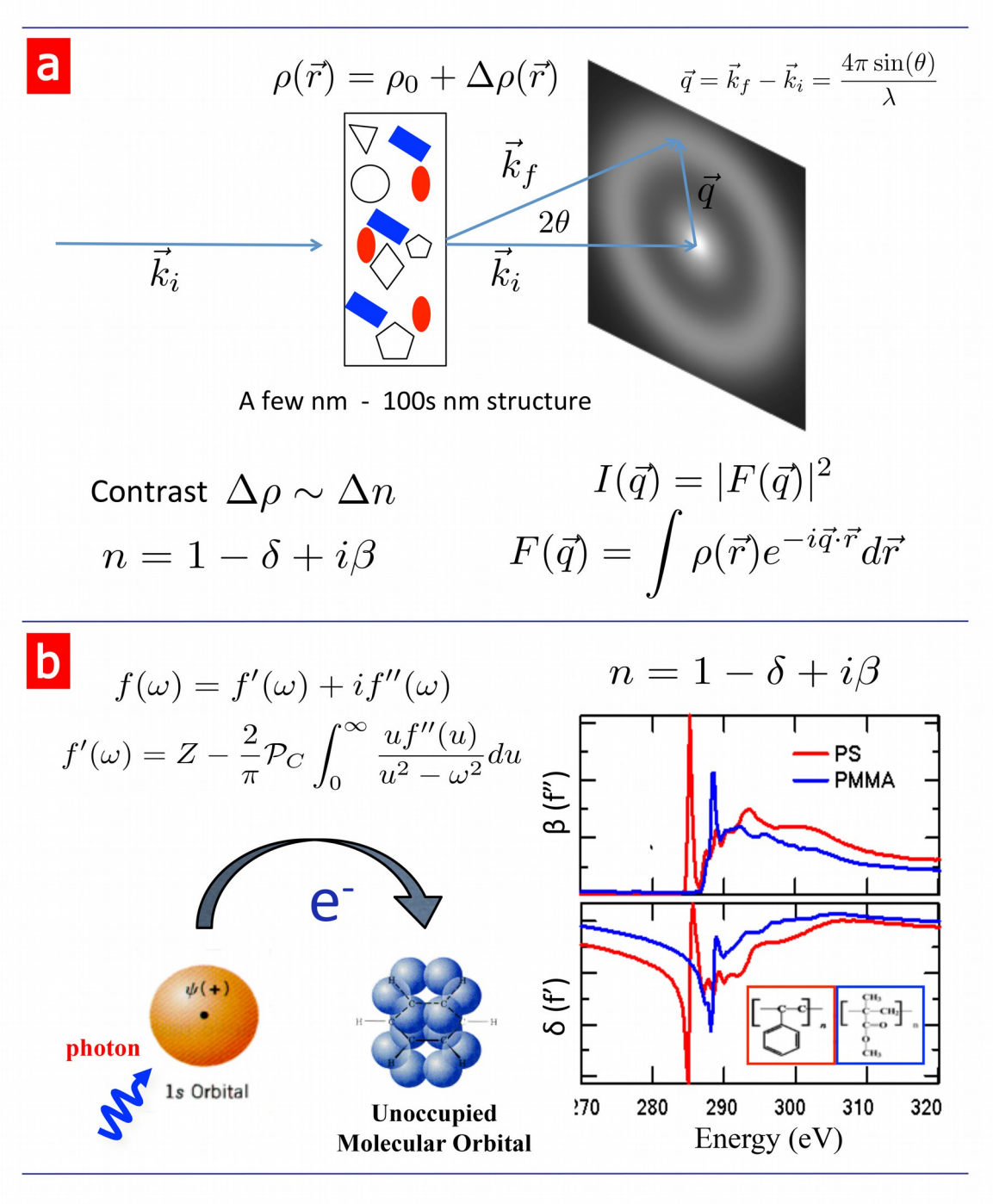

Figure 1 (a) Schematic summary of conventional transmission SAXS, with the scattering contrast related to the complex index of refraction. **(b)** The fundamental relations and physical mechanism exploited in anomalous scattering and energy dependent δ and β for polystyrene (PS) and poly(methyl methacrylate) (PMMA).

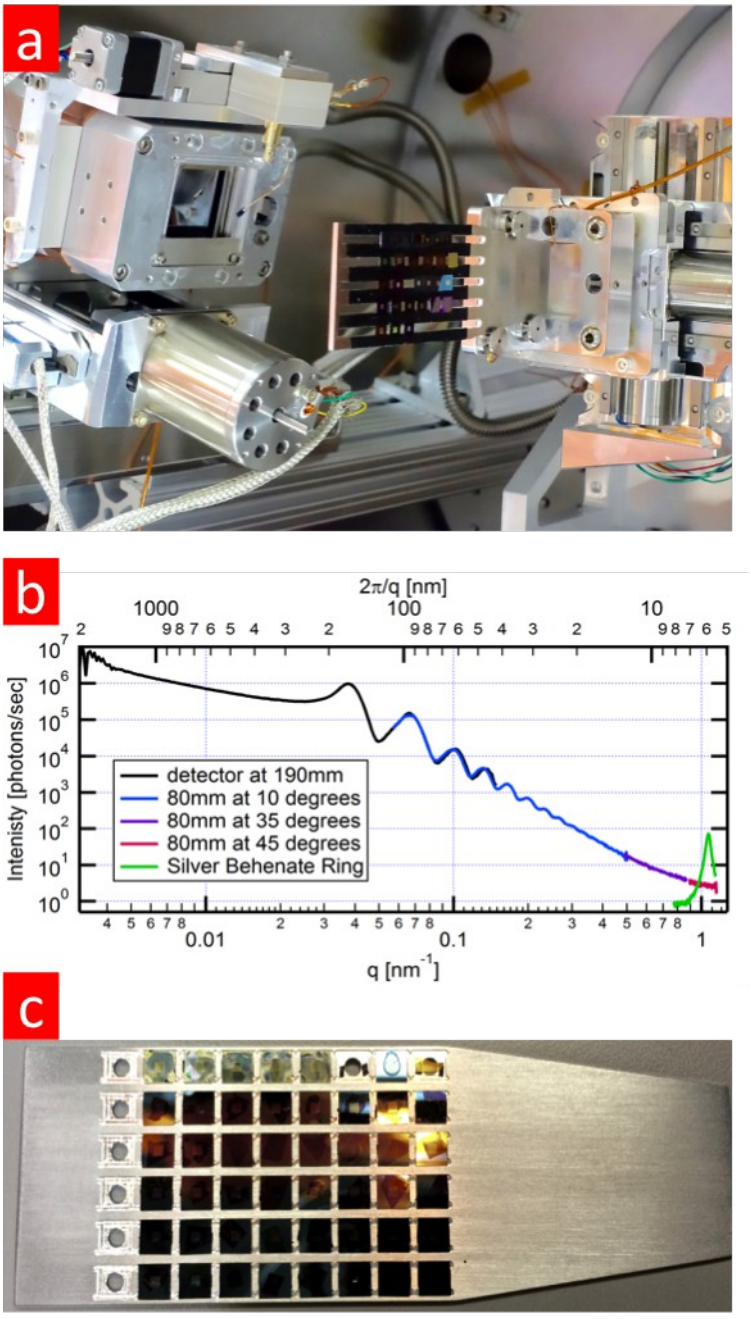

Figure 2 (a) Photograph of the RSoXS scattering chamber, with CCD detector at left and sample plate in center. Importantly, the chamber provides flexibility for customizable sample environments. **(b)** RSoXS pattern for a calibration sample of 300 nm diameter PS spheres in latex, mostly highlighting the very large *q* range accessible by movement of the sample-detector distance and detector tilt. Length scales from 5 nm to 2 □m can

be routinely investigated. **(c)** Photograph of the sample holder plate that is capable of high-throughput, in-situ, and electrical biasing RSoXS experiments. Partially adapted from Ref. 20.

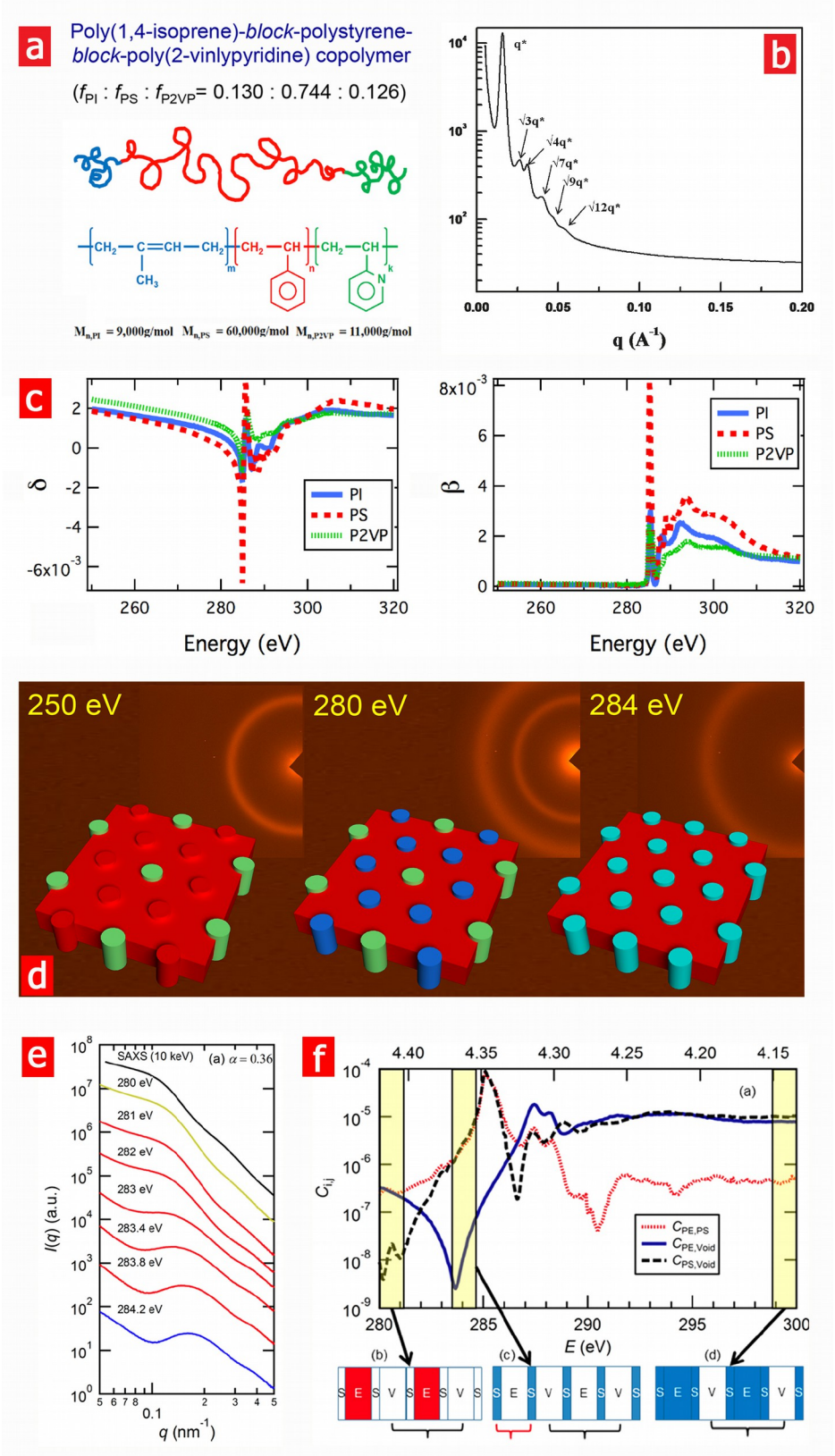

Figure 3 (a) Chemical formula, composition, and molecular weight of the PI-*b*-PS-*b*-

P2VP block copolymer investigated in Ref. 26. **(b)** Hard x-ray SAXS shows a hexagonally packed cylindrical structure. **(c)** The real, dispersive and imaginary, absorptive components of the complex index of refraction of PS, PI and P2VP. **(d)** Energy dependent RSoXS images showing the nested hexagonally packed domain structure. **(e)** and **(f)** Hard and soft x-ray SAXS and a schematic showing the void and polymer domain structure in a SES triblock copolymer. Adapted from Refs. 26, 32, and 33.

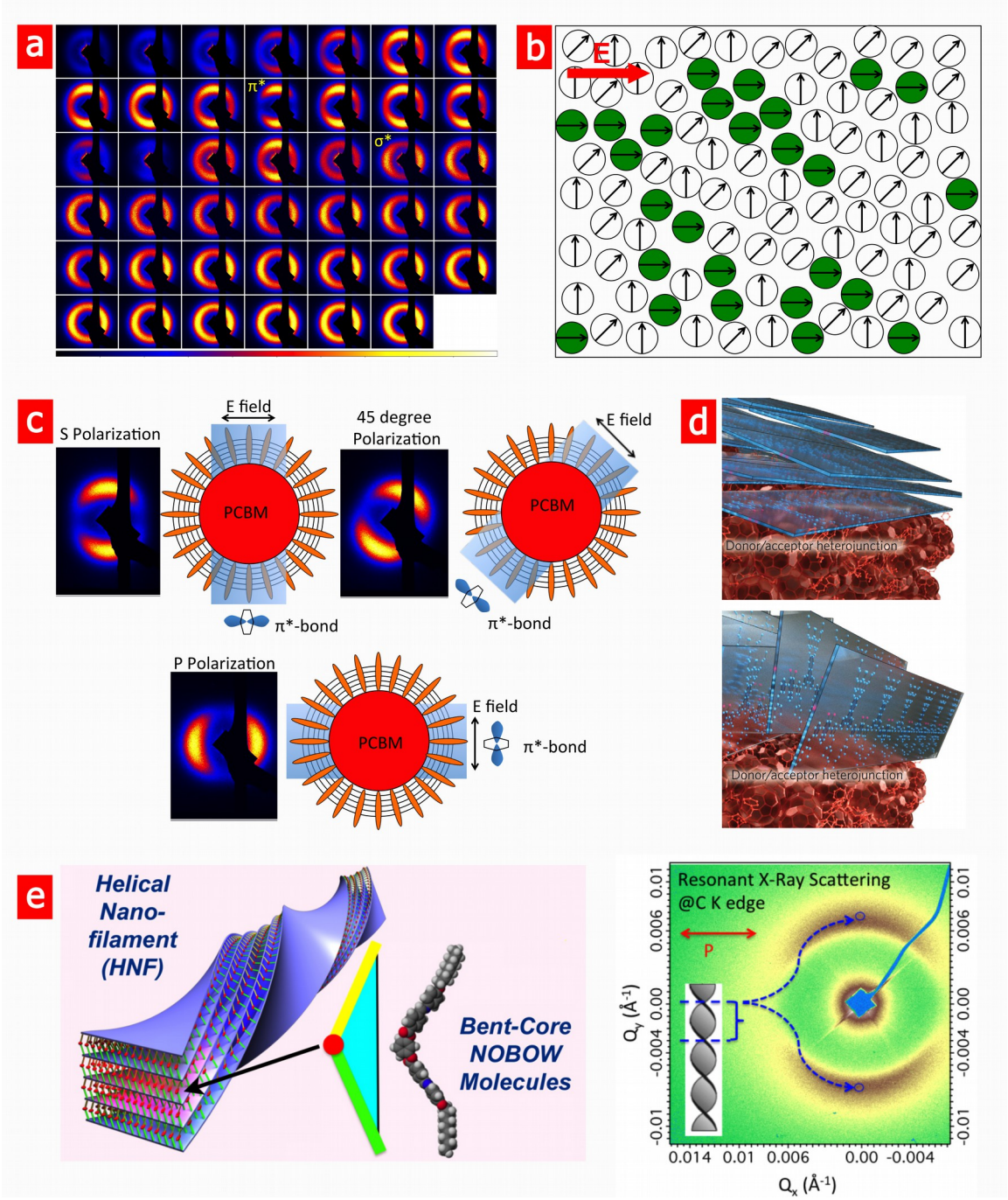

Figure 4 (a) Energy dependent transmission RSoXS images of DPP:PCBM blends across the carbon 1s edge, showing anisotropy near π* and σ* transitions. **(b)** Schematic displaying the selective excitation of horizontally oriented molecular transition dipole moments with the horizontally oriented electric field of the incident x-rays. **(c)** and **(d)** Polarization dependent scattering patterns from DPP:PCBM blends and cartoons explaining the local molecular orientation information that these patterns

contain. **(e)** Helical structure of filaments of liquid crystalline NOBOW (shown in inset) and the RSoXS image that shows scattering from the pitch spacing of the helix. Adapted from Refs. 42 and 43.

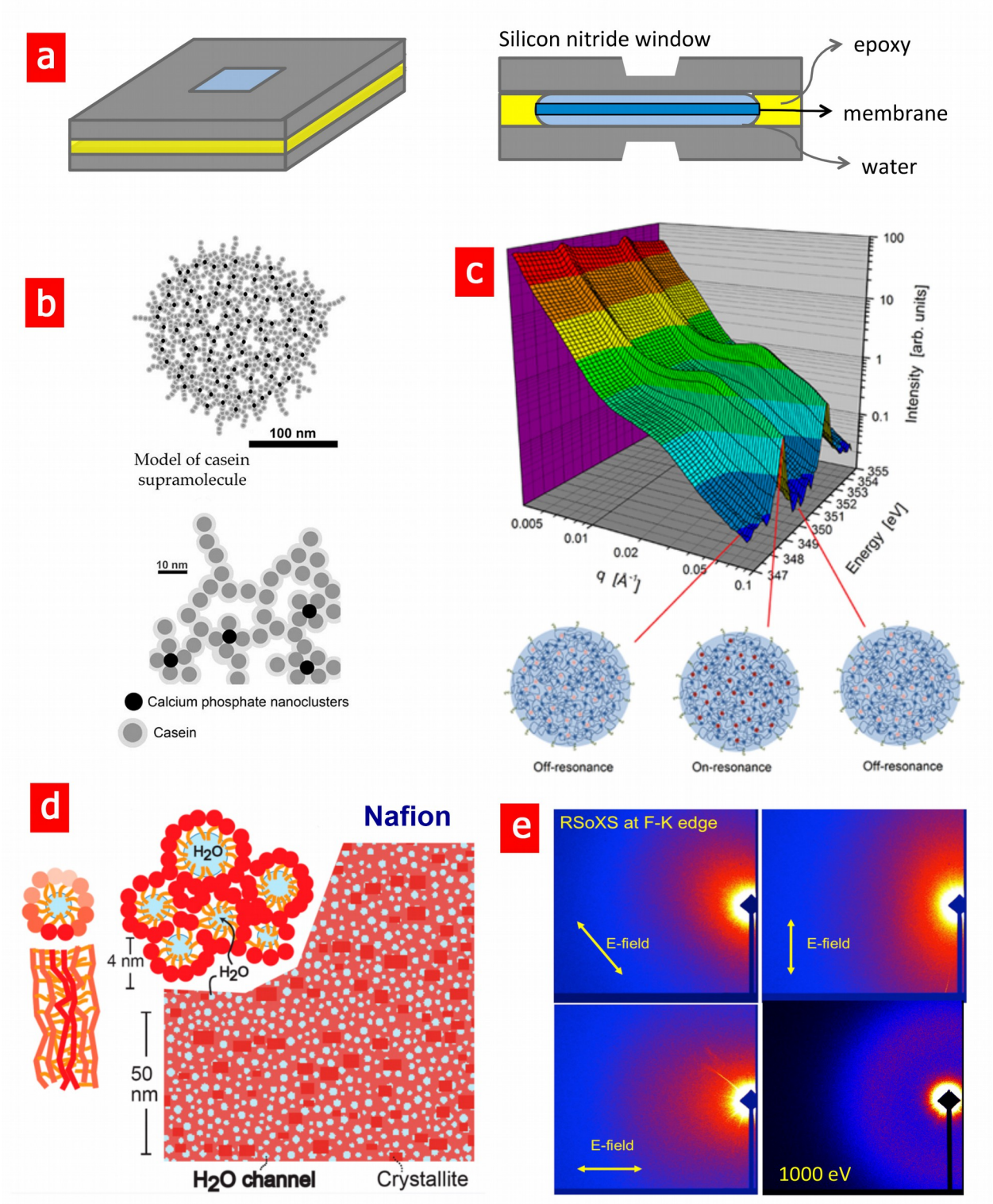

Figure 5 (a) Diagrams of the solution cell created by joining two silicon nitride window substrates. In this case, a membrane sample in water is shown on the right. **(b)** and **(c)** Hierarchical colloidal structure of the casein macromolecule in milk. The Ca L edge

scattering shows that the calcium phosphate nanoclusters are contained within the casein globules. **(d)** Nafion has a hierarchical organization that becomes swollen with water. **(e)** Scattering at the fluorine K edge reveals its local molecular orientation in these water channel domains. Partially adapted from Ref. 46.

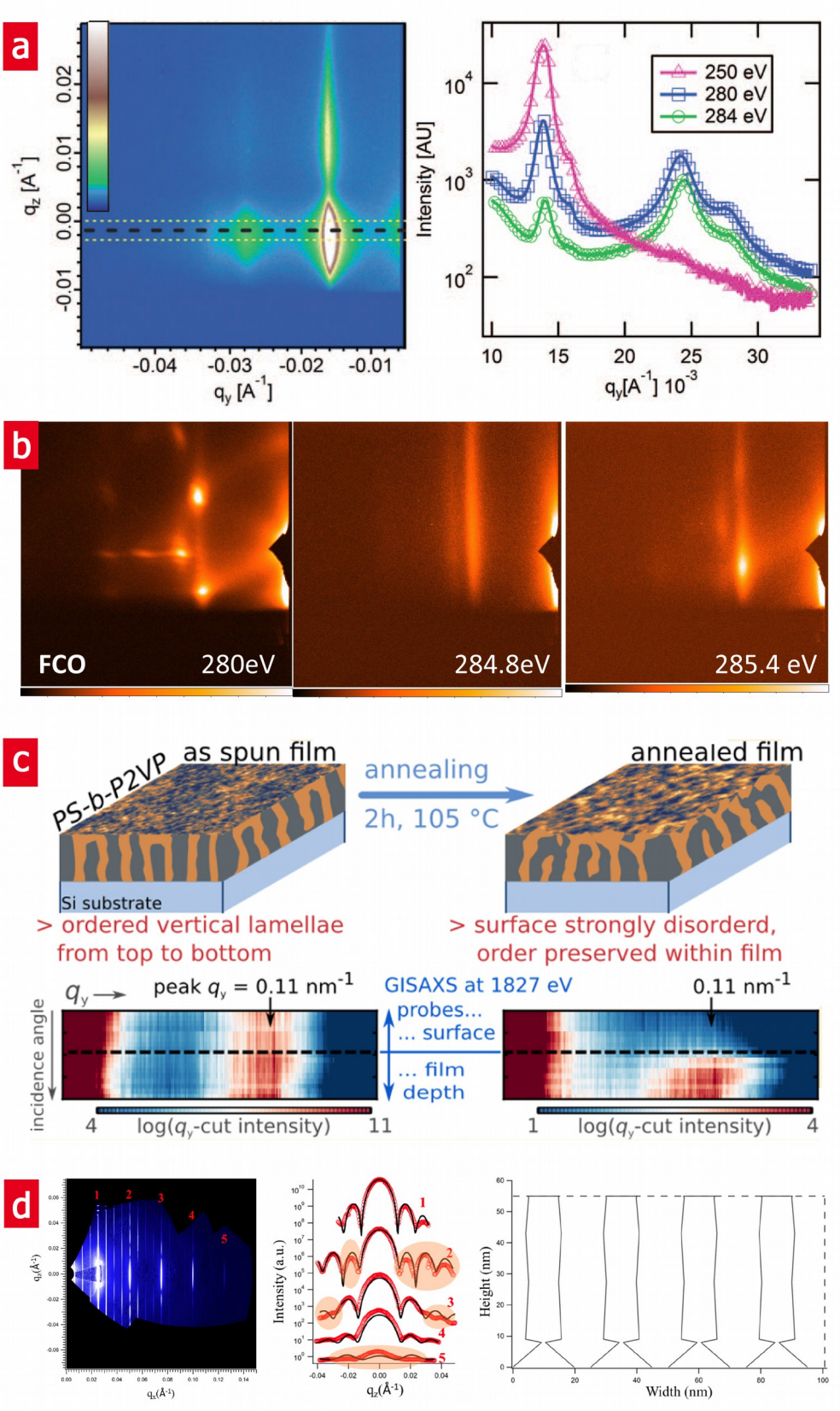

Figure 6 (a) GI-RSoXS imaging and reduced patterns from an IS2VP triblock copolymer

thin film. **(b)** GI-RSoXS imaging of a mesoporous block copolymer thin film at three different energies. **(c)** Thermal annealing drives surface disordering in thin films of PS-*b*-P2VP as found by GI-RSoXS. Surface and buried structures can both be probed by selecting the appropriate energy and incident angle. **(d)** CD-SAXS with soft x-rays enables the 3-D investigation of domain structure in thin films of self-assembled block copolymers. Partially adapted from Refs. 56 and 57.